JOURNAL OF MATERIALS SCIENCE **38** (2003) 3257–3262

Grain size dependence of mechanical, corrosion and tribological properties of high nitrogen stainless steels

A. DI SCHINO
Materials Engineering Center, University of Perugia, 05100 TERNI, Italy

M. BARTERI
Centro Sviluppo Materiali, Viale B. Brin, 05100 TERNI, Italy

J. M. KENNY*
Materials Engineering Center, University of Perugia, 05100 TERNI, Italy
E-mail: kenny@unipg.it

Austenitic stainless steels have been indispensable for the progress of technology during the last 80 years. Due to the cost of nickel and to the prospective of allergic reactions caused by this element, more and more laboratories and industries are trying to develop a new class of austenitic stainless steels with a low nickel content. In order to maintain the austenitic microstructure, nickel reduction is balanced with nitrogen addition. Nitrogen addition to austenitic stainless steels is also very effective for improving yield strength and corrosion resistance without reducing ductility and toughness. In order to further increase the strength, it is possible to combine the effect of nitrogen addition and grain refining. The purpose of this study is to examine the relationship between microstructures and mechanical, corrosion and tribological properties of a high nitrogen stainless steel with an ultrafine grained structure.

1. Introduction

Nitrogen alloyed austenitic stainless steels exhibit attractive properties such as high strength and ductility, good corrosion resistance and reduced tendency of grain boundary sensitization [1]. The high austenitizing potential of nitrogen allows the nickel content in the steel to be reduced, offering additional advantages such as cost savings. The production of these low nickel steels is made possible by the addition of manganese that allows the increase of N solubility in the melt and decreases the tendency of Cr_2N formation [2].

Although there have been many studies on finely grained ferritic steels (e.g. [3]), only a few research reports are available on refined austenitic stainless steels. The grain size of ferritic steels can be easily refined by phase transformation, but in austenitic alloys, due to the absence of phase transformation, the grain diameter is usually controlled by recrystallization after cold working [4]. This method is affected mainly by the working temperature, reduction and recrystallization temperature. Recrystallization after hot rolling is reported to have the effect of grain refining but this method seems to be limited [5].

In previous papers [6, 7], we examined the effect of subzero working on the grain refining of austenitic stainless steels. In particular, ultrafine grained AISI 304 stainless steel with an average grain size of ca. 0.8 μm was obtained by applying the reverse transformation of martensite to austenite, in subzero-worked steel, annealed at low temperatures. Furthermore, a strong increase was found both in the mechanical [6] and in the localised corrosion [8] resistance.

In order to further increase the strength, it is possible to combine the effect of nitrogen addition and grain refining. Due to the absence of high temperature phase of this class of stainless steels [9], the only way to promote grain refining seems to be dynamic recrystallization in hot working or static recrystallization after cold rolling and subsequent annealing.

The purpose of this study is to examine the relationship between microstructure and mechanical properties of a high nitrogen austenitic stainless steel (hereinafter referred to as HN) with ultrafine grained structures obtained by means of cold rolling and subsequent annealing.

2. Materials and experimental details

The chemical composition of the HN stainless steel, considered in this work, is shown in Table I. Industrial hot rolled and annealed samples (50×200 mm), whose thickness was 3 mm, were cold rolled using different

* Author to whom all correspondence should be addressed.

TABLE I Chemical composition of high nitrogen steel (mass %)

Cr	Ni	Mn	Cu	Si	Mo	N	P	S	C
18.5	1.07	11.4	1.07	0.12	0.08	0.37	0.022	0.003	0.037

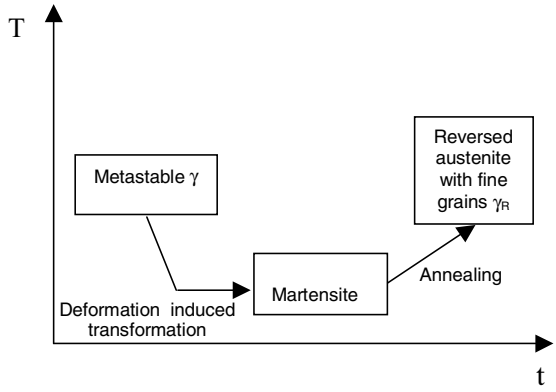

Figure 1 Thermo mechanical treatment adopted to obtain an ultrafine structure by martensitic reversion.

thickness reductions (from 5% to 75%). The grain size before cold reduction was approximatively 25 μm.

In order to analyse the effect of cold rolling temperature on martensite formation the following procedure has been carried out (Fig. 1). Cold reduction was carried out at two different temperatures: in the first case specimens were rolled after cooling in liquid nitrogen (about $-$°C), in the latter they were deformed without no prior cooling (room temperature). In both cases martensite content was measured after deformation by ferritoscope. Deformation and martensite content were considered homogeneous within the samples. Quenched and cold rolled samples were then annealed at different temperatures (in the range 700°C to 1100°C), in order to investigate the martensite-austenite reversion. Samples were analysed after austenite reversion and automatic image analysis has been used for the measure of grain size.

Furthermore, in order to investigate the effect of grain size on mechanical properties of the steel, longitudinal ISO 50 tensile test specimens were cut from samples corresponding to different annealing conditions. Tensile tests were carried out with a deformation rate of 3 mm/min. The hardness of the steels was determined using a microhardness tester equipped with a Vickers indenter at a load of 500 g.

In order to analyse the grain size effect on the corrosion resistance, steel materials were machined to corrosion test specimens of 15 $\times$ 15 $\times$ 1 mm. The specimen surface was polished by using increasingly finer abrasive papers, starting from 300 grit paper and finishing with 4000 grit paper. They were then immersed in different solutions and corrosion was measured by the weight loss after the test.

Potentiodynamic polarisation tests were carried out at 25°C in a conventional glass cell using a deareated 35 g/l NaCl solution as electrolyte. The potential of the working electrode was measured using a saturated calomel electrode (SCE) as reference. The counter electrode was a platinum foil. The scan rate was 2.4 V/h. Before starting, a cathodic reduction of the passive film was performed at -1 V/SCE for 90 s. The pitting potential values, E_p, were taken as the last value at which the current was as low as that of a completely passive specimen. Each specimen was subjected to a minimum of three complete scans.

Friction and wear determinations were made using a Ball-on-Disk (BoD) tribometer with a 6 mm diameter 100Cr6, hard metal and sapphire balls at a normal load of 2 N and a speed of 10 cm/s and at room temperature and a relative humidity of 50%. The wear track was measured after each experiment using a diamond stylus profilometer. The scratch resistance was observed with a nano scratch tester with a 20 μm diamond indenter starting from 5 mN to 30 mN at 10 mm/min for a total scratch length of 2 mm. This testing was also done at room temperature and at a relative humidity of 50%.

3. Results and discussion

The curves relating the martensite content M to the true strain ε, are shown in Fig. 2 for the cooled and deformed steel and for the steel deformed without prior cooling. In the cooled and deformed steel about 45% of γ is transformed into martensite using 75% reduction ($\varepsilon = 0.52$) deformation ratio, while, in the steel rolled without cooling, only 12% of martensite is produced after 75% cold reduction. Results of similar measurements on a standard AISI 304 [6] showed that for this steel at the same deformation ratio, about 80% of martensite was obtained after cooling at -100°C and cold rolling. The lower martensite content in the high nitrogen steel is due to the addition of Mn and N that stabilizes austenite against strain induced martensite formation. Only the sample deformed at 75% after cooling in liquid nitrogen was subjected to reversion treatment because grain refinement increases with martensite content [6].

In order to check the reversion kinetics, this sample was annealed at different temperatures (700°C to 1100°C) and times (10 s to 100 ks). Fig. 3 shows the evolution of reversed martensite volume fraction as a function of annealing time and annealing temperatures. The dotted lines connect the data to the initial martensite volume fraction (45%). It can be observed that,

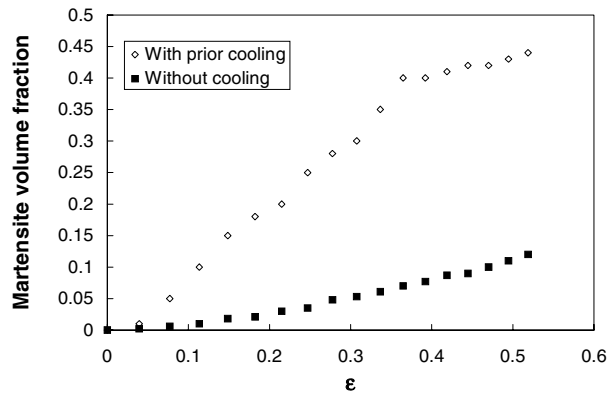

Figure 2 Formation of martensite by cold rolling with and without prior cooling in liquid nitrogen.

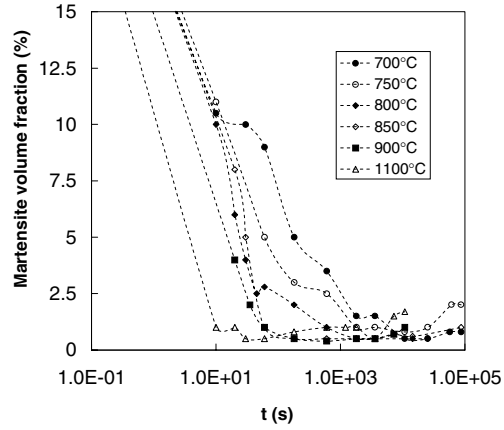

Figure 3 Effect of annealing time and temperature on reversion behaviour of martensite.

as expected, the martensite volume fraction decreases as time increases and the martensite reversion rate increases with the annealing temperature. Fig. 3 can be used to determine the martensite-austenite reversion kinetics for this material. The effect of annealing temperatures and times on the grain size is shown in Fig. 4.

Results show that at 900°C, even for long annealing times, no significant grain growth takes place. The grain size varies from 2.4 μm after 10 s of annealing time to 3 μm after 10 ks. Further measures at lower annealing temperatures show that also in these cases the minimum obtainable grain size is about 2.4 μm. This can be explained assuming that the minimum austenite grain size just depends on the number of nuclei per unit volume induced by deformation. Since all the samples come from the same cold rolled steel, they will have the same number of nuclei before annealing, and then show the same recrystallized grain size. On the contrary, as expected, thermally activated grain growth occurs for $T = 1100$°C and grain size quickly increases. In Fig. 5 the microstructure of the sample annealed at 900°C for 600 s is shown, and in Fig. 6 its grain size distribution, measured by automatic image analyzer, is shown.

Grain refinement is commonly known to increase the hardness and the strength of grained materials. It is well recognized that the yield stress R_{p02} and the hardness HV of a metallic material increase with decreasing grain size d.In particular, the Hall-Petch equation expresses the grain-size dependence of strength and micro hardness [10, 11]. In terms of strength and hardness, the Hall-Petch equations are:

$$R_{p02} = R^0_{p02} + kd^{-1/2} \quad (1)$$

$$H = H_0 + k'd^{-1/2} \quad (2)$$

where the superscript 0 relates to the material of infinite grain size; $k$and k' are constants representing the grain boundary as an obstacle to the propagation of deformation.

The effect of grain size on tensile properties is shown in Figs 7 and 8, where also similar measurements on

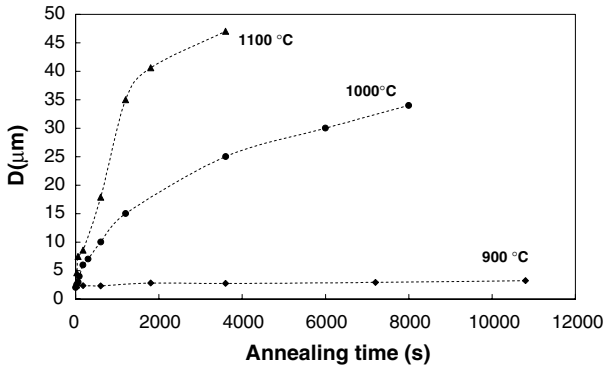

Figure 4 Effect of annealing temperatures and times on grain size.

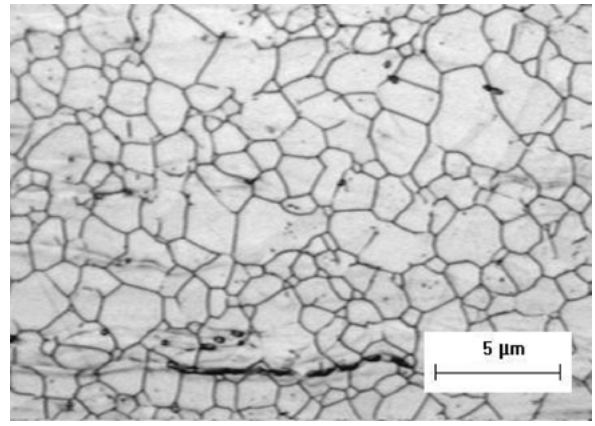

Figure 5 Microstructure of HN steel annealed at 900°C for 600 s.

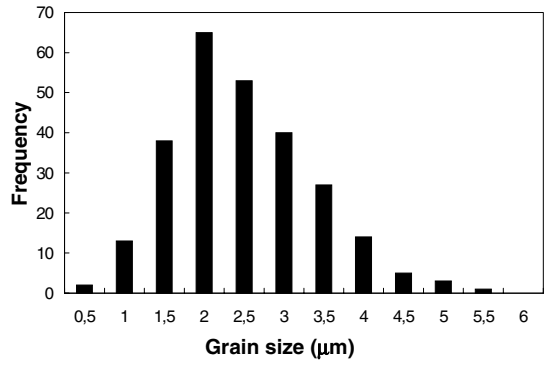

Figure 6 Grain size distribution of HN steel annealed at 900°C for 600 s.

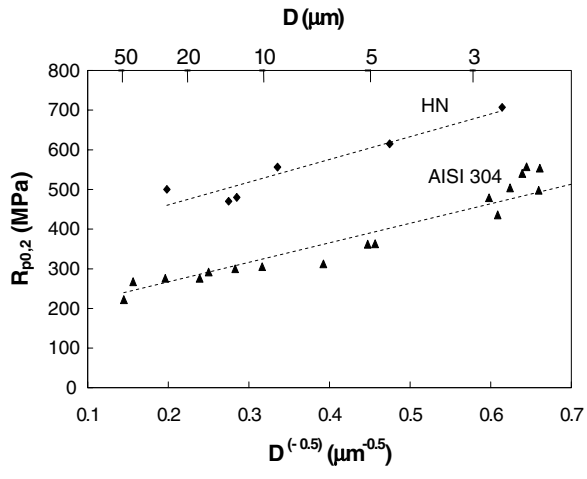

Figure 7 Dependency of the yield strength on grain size of high nitrogen and AISI 304 stainless steels.

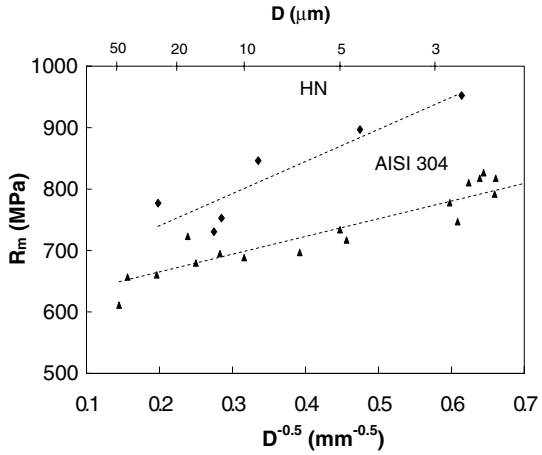

Figure 8 Dependency of the tensile strength on grain size for high nitrogen and AISI 304 stainless steels.

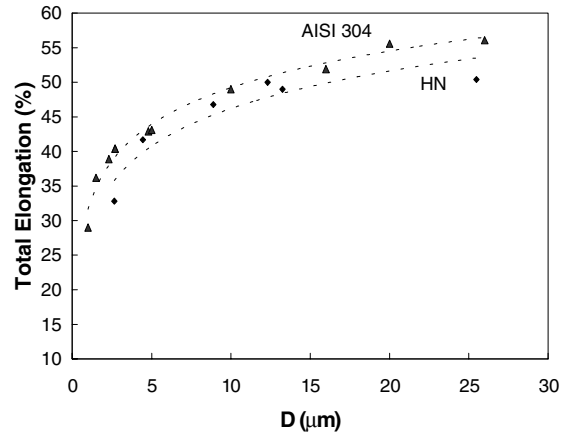

Figure 10 Grain refinement effect on the ductility of high nitrogen steel compared to AISI 304 stainless steel.

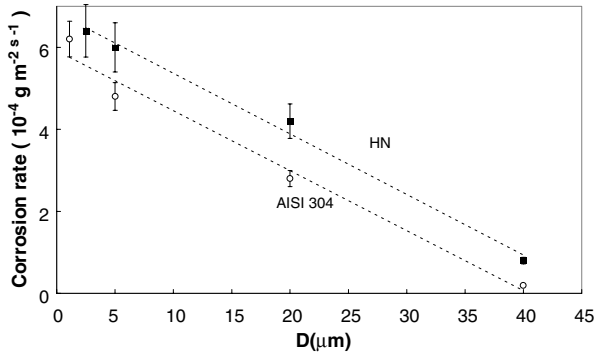

Figure 11 Relation between the general corrosion rate in boiling 5% H_2SO_4 solution and the average grain size.

a standard AISI 304 stainless steel are reported. The positive effect of nitrogen addition in increasing the steel strength for a given grain size is outlined; furthermore, grain size effect in strengthening is observed for both steels. In particular, the Hall-Petch dependency for both yield stress (R_{p02}) and tensile strength (R_m) is found to be valid for the examined grain size ranges for both high nitrogen steel and AISI 304 stainless steel. In Fig. 9 hardness versus the inverse square root of grain size is reported for both the high nitrogen and the AISI 304 stainless steels. Finally, Fig. 10 shows that the ductility of the high nitrogen steel is slightly lower than that of the AISI 304 stainless steel. Total elongation is reduced when grain size is refined in both steels.

The general corrosion (GC) rate of the HN stainless steel with 2.5 to 40 μm grain sizes was measured in 5% H_2SO_4 boiling solution for 36 ks, and the results are shown in Fig. 11. The corrosion rate of HN steel increases with decreasing grain size. Since an higher concentration of manganese oxides was detected by Scansion Electron Microscopy at grain boundaries with respect to the matrix, these results can be interpreted in terms of defects concentrated in grain boundaries; then, increasing the grain boundary surface area by grain refining seems to cause passive film destabilization, and thus ultrafine-grained steels show a reduction of the general corrosion resistance. Furthermore the GC rate of the HN steel is higher than that of the standard AISI 304 steel; this can be explained in terms of higher inclusion density in HN with respect to AISI 304 steel, due to Mn alloying, as confirmed by an investigation with the Scanning Electron Microscopy.

To estimate the intergranular corrosion rate (IGC) of HN, steel samples were immersed in H_2SO_4-$FeSO_4$ (Streicher solution) for 36 ks; the weigth loss related to time and surface unit was taken as a measure of the IGC resistance (results in Fig. 12). The corrosion rate

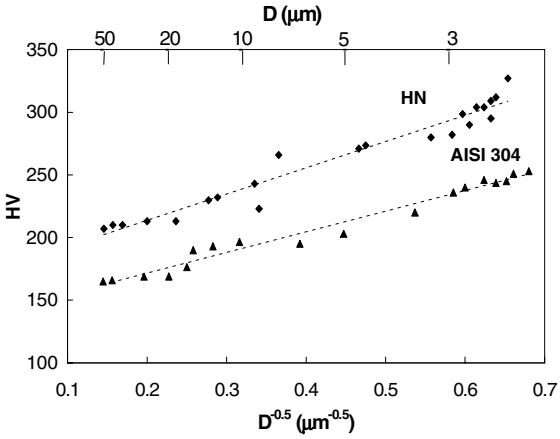

Figure 9 Dependency of the hardness on grain size of high nitrogen and AISI 304 stainless steels.

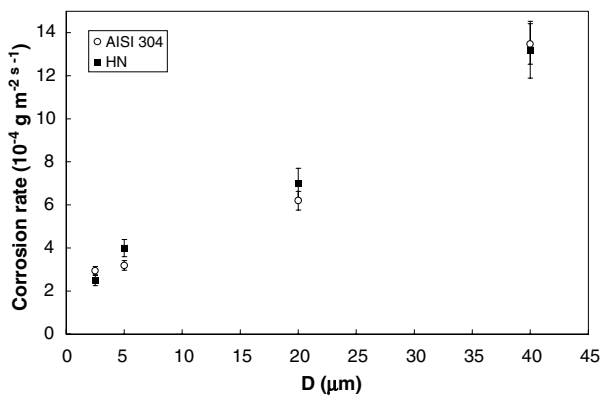

Figure 12 Relation between the intergranular corrosion rate in boiling Stericher solution and the average grain size.

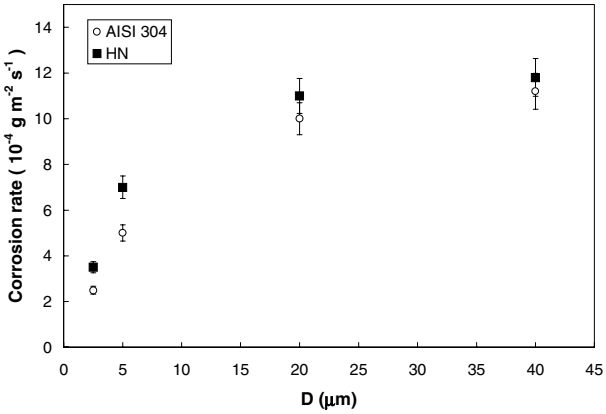

Figure 13 Relation between the pitting corrosion rate in 10% $FeCl_3$-$6H_2O$ solution and the average grain size.

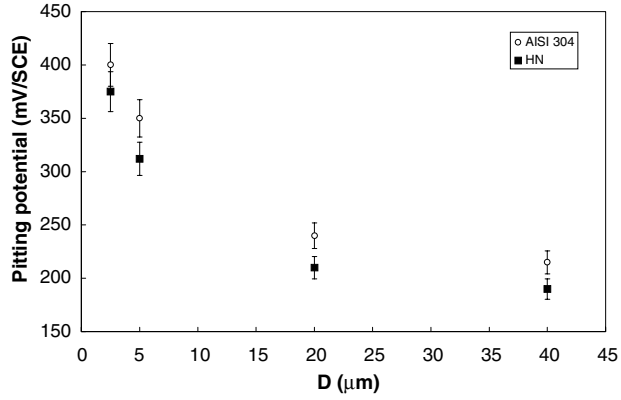

Figure 14 Relation between the pitting potential E_p in 3.5% NaCl solution at 303 K and the average grain size.

decreases with decreasing grain size. As inter-granular corrosion is caused by the precipitation of carbides in grain boundaries, the corrosion rate is affected by the volume fraction of precipitated carbides per unit of grain boundary area. As grain size is refined, the grain boundary areas per unit volume increase and the degree of the Cr depletion caused by carbide precipitation will decrease for a given C content. Hence, boundaries may not be sensitised in finely grained materials. Furthermore, the IGC rate of the HN steel is comparable to that of the AISI 304 steel, the Cr and C contents being almost the same in both steels (see Table I). The pitting corrosion rate (PC) rate of HN steel was measured in a 10% $FeCl_3$-$6H_2O$ solution at room temperature for 36 ks, and the results and comparison to standard AISI 304 steel are shown in Fig. 13. The PC resistance of the HN steel is lower than that of the AISI 304 steel: also, in this case, this result can be explained in terms of a higher inclusion density in the HN steel with respect to the standard steel. In particular, manganese oxides (due to the high Mn content in the HN steel) have been detected by Scansion Electron Microscopy. Furthermore, in contrast to the reduction of the general corrosion resistance, the grain refining leads to an improved pitting corrosion resistance in both steels. Optical microscopy observations revealed that the pitting of coarsely grained steel initiates in limited sites, with large and deep individual pits. In contrast, the pitting of ultrafine grained steel initiates in several sites, but with small individual pits; the increase of pitting corrosion sites number in the ultrafine grained steel leads to a decrease of anodic current density with respect to the corsely grained steel. In particular an average current density of about 0.1 μA/cm^2 and 0.4 μA/cm^2 was measured in the ultrafine and in the corsely grained steel, respectively, with a consequent beneficial effect of grain refining on the pitting corrosion resistance.

To confirm this result, the pitting corrosion resistance was also analyzed by potentiodynamic polarisation tests. As shown in Fig. 14, the pitting potential shifts towards more noble potentials with decreasing grain size, according to the corrosion data.

The tribological behaviour in BoD tests (Fig. 15) shows that the grain size has little effect upon the friction coefficient. Testing was performed under dry

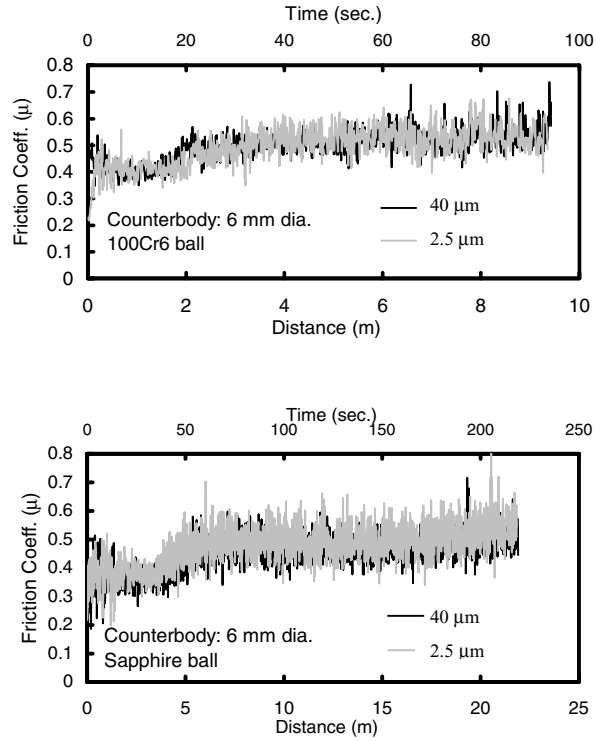

Figure 15 Friction-Distance-Time graphs of HN stainless steel with different grain size.

conditions and for a short time to determine the initial friction coefficient. Similarly, changing the counter body also does not affect the friction coefficient value, which for the entire testing time period remained stable at around 0.5, which corresponds to friction coefficient value of steel against steel (0.6 to 0.7). The wear behaviour shows some differences and here for all counterbody materials, the finest grained steel shows itself to be more wear resistant than the large grain steel (Fig. 16). The wear rate of 100Cr6 and hard metal against both steels is almost identical, while tests with a sapphire counter body show has a slightly reduced wear rate for both samples with 2.5 and 40 μm grain size. Differences are also observed in the scratch resistance using a diamond indenter, with 2.5 μm grained steels exhibiting more scratch resistant than the 40 μm grain size steels. This is evident from the lower penetration depth of the fine grained steels in nano

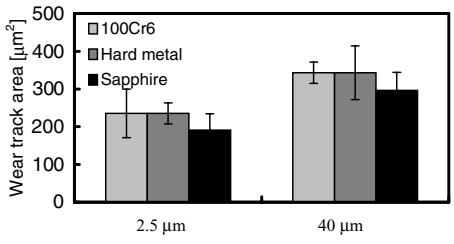

Figure 16 Wear Track Area-Grain size for HN austenitic stainless steel.

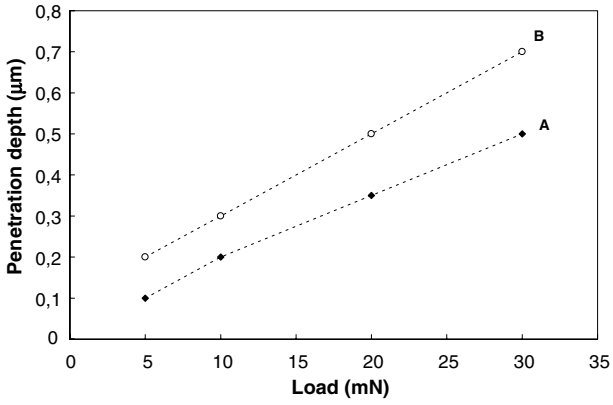

Figure 17 Penetration Depth-Load graphs for HN austenitic stainless steel with 2.5 (A) and 40 (B) grain sizes.

scratch tests (Fig. 17). This is attributed to the increased yield strength as well as higher hardness of the fine grain steels.

4. Conclusions

In this paper grain refinement was applied to high nitrogen content austenitic stainless steels and the effect of grain size upon the mechanical as well as corrosion and tribological behavior was examined. The austenitic-martensite-austenitic transformation by deformation and annealing treatment resulted in a steel with an average grain size as small as 2.5 μm. The mechanical characterization of the austenitic steels with different grain sizes showed that the microhardness increases with decreasing grain size, as does the yield and flow stress; however a slight decrease in the ductility was also observed with decreasing grain size. From the corrosion tests, it can be drawn out that both the inter-granular and pitting corrosion rate decreases with decreasing grain size while the general corrosion resistance is impaired by grain refining. Tribological testing showed that grain refinement has little effect upon the friction behavior. However, the fine-grained steels appear to be more wear resistant and also have a higher scratch resistance.

References

1. A. RECHSTEINER and M. SPEIDEL, in Proc. of the 1st European Stainless Steel Conference (Florence, 1997) Vol. 2, p. 107.
2. A. DI SCHINO, J. M. KENNY, M. G. MECOZZI and M. BARTERI, *J. Mater. Sci.* **35** (2000) 4803.
3. K. KIYOSHIGE and S. PYUSUKE, *Jpn. Inst. Met.* **44** (1980) 1037.
4. R. E. REED-HILL, "Physical Metallurgy Principles" PWS Publishing Company (1994).
5. I. SALVATORI, T. HAYASHY and K. NAGAI, in Proc. of the Int. Workshop on Innovative Structural Materials (Tsukuba, 2000) p. 24.
6. A. DI SCHINO, J. M. KENNY and I. SALVATORI, in Proc. of the 4th European Stainless Steel Conference (Paris, 2002) Vol. 2, p. 22.
7. A. DI SCHINO, J. M. KENNY and M. BARTERI, *J. Mater. Sci. Lett.* **21** (2002) 751.
8. A. DI SCHINO and J. M. KENNY, *J. Mater. Sci. Lett.* **21** (2002) 1631.
9. M. SPEIDEL, in Proceedings of the 5th International Conference on High Nitrogen Steels (Stockolm, 1998) p. 241.
10. E. O. HALL, *Proc. Phys. Soc.* **64B** (1951) 747.
11. N. J. PETCH, *J. Iron & Steel Inst.* **174** (1953) 25.

Received 12 September 2002
and accepted 22 April 2003